

Estimation of the macromolecular proton fraction and bound pool T_2 in multiple sclerosis

Davies GR¹, Tozer DJ¹, Cercignani M¹, Ramani A¹, Dalton CM¹, Thompson AJ¹, Barker GJ^{1,2}, Tofts PS¹ and Miller DH^{*1}

¹NMR Research Unit, Institute of Neurology, UCL, Queen Square, London WC1N 3BG, UK; ²Neuroimaging Research Group, Box 042, Institute of Psychiatry, De Crespigny Park, London SE5 8AF, UK

This study used a model for magnetization transfer (MT) to estimate two underlying parameters: the macromolecular proton fraction (f) and the bound pool T_2 (T_{2b}) in patients with multiple sclerosis (MS). Sixty patients with clinically definite MS and 27 healthy controls were imaged using: (1) a dual echo fast spin echo sequence, (2) a MT sequence (with ten MT power and offset frequency combinations) and (3) proton density and T_1 weighted sequences (for T_1 relaxation time estimation). Fourteen normal-appearing white matter (NAWM) regions of interest (ROI) and six normal-appearing gray matter (NAGM) ROIs were outlined in all subjects. Lesions were also contoured in subjects affected by MS. The model was fitted to the data leading to estimates of T_{2b} and f . Results showed that T_{2b} was increased in lesions whereas f was reduced. In NAWM, f was decreased while T_{2b} was only increased in secondary progressive MS. NAWM f correlated modestly with disability. Further studies are needed to investigate the pathological basis of the abnormalities observed. Multiple Sclerosis (2004) 10, 607–613

Key words: magnetization transfer ratio; multiple sclerosis; normal appearing white matter; gray matter; lesions; myelin

Introduction

Magnetization transfer (MT) is a technique that has been used widely in the study of multiple sclerosis (MS), particularly as it provides an indirect assessment of the macromolecular content of a tissue.^{1–4} In the central nervous system, phospholipid bilayers may comprise much of the macromolecular proton content,^{1,5} and this may explain why the MT ratio (MTR) correlates with both axonal and myelin density.⁶ Although MTR is abnormal in MS pathology, it is not specific for any single pathological feature,^{6,7} and it is possible that further insights will be obtained by estimating the parameters that underlie the MT effect. These parameters include the macromolecular proton fraction (f) and the T_2 relaxation time of the bound pool (T_{2b}).

A mathematical model for the magnetization transfer effect based on two pools of protons has previously been proposed by Henkelman *et al.*⁸ The first pool comprises protons in free water with the second representing protons within macromolecules. The model relates the magnetization of the partially saturated free water to the relative size of the two pools, acquisition specific parameters (including the offset frequency and amplitude of the saturating

MT pulse) and a number of relaxation and absorption rate constants. Our adaptation of this technique has permitted f and T_{2b} to be estimated in human subjects,^{9,10} by fitting our model to experimental data. Similar techniques have been developed by Sled and Pike,¹¹ and Yarnykh,¹² but whereas these permit *in vivo* parameter estimation in a single slice, our technique, is able to provide whole brain coverage^{9,10} which would be helpful in a diffuse and multifocal disease process such as MS.

We report our findings applying this technique in 60 patients with MS. The aims of this study were: (1) to investigate whether abnormalities of f and T_{2b} are present in MS lesions and normal appearing tissues and, (2) to explore the relationship of the new measures with clinical status.

Methods

Subjects

Sixty subjects with clinically definite MS,¹³ (38 female and 22 male; mean age 47 years, range 27 to 73 years; 27 with relapsing remitting (RRMS), eight with benign (BMS), 12 with primary progressive (PPMS) and 13 with secondary progressive MS (SPMS),¹⁴) and 27 healthy control subjects (13 female and 14 male; mean age 35 years, range 23 to 52 years) were studied (Table 1). As there was a large age difference between controls and the MS group, comparisons between MS patients and controls were made using only those patients aged less than 50. The demographics of this subset were as follows: 18 female, 15 male; mean age 39, range 27 to 50 years; 22

*Correspondence: Professor DH Miller, NMR Research Unit, Institute of Neurology, Queen Square, London, WC1N 3BG, UK.

E-mail: d.miller@ion.ucl.ac.uk

Received 21 January 2004; revised 8 April 2004; accepted 21 June 2004

Table 1 EDSS and disease duration in the full patient cohort and in the four clinical subgroups

	N	Median EDSS (range)	Mean disease duration/years (range)
Full MS cohort	60	3.0 (1.0–7.5)	15 (0.5–38)
Relapsing–remitting MS	27	2.0 (1.0–5.0)	9 (0.5–27)
Benign MS	8	2.5 (2.0–2.5)	23 (19–32)
Secondary progressive MS	12	6.0 (3.5–7.5)	24 (5–38)
Primary progressive MS	13	6.0 (2.0–7.0)	12 (9–21)

with RRMS, one with BMS, six with SPMS and four with PPMS. In subjects affected by MS, the expanded disability status scale (EDSS) score,¹⁵ and the MS functional composite scores (MSFC),¹⁶ were determined.

The study was approved by the joint ethics committee of the Institute of Neurology and the National Hospital for Neurology and Neurosurgery. All subjects gave informed written consent prior to the study.

MRI acquisition

Imaging was performed on a 1.5 Tesla Signa scanner (General Electric, Milwaukee, USA). Three sequences were acquired in all subjects. (1) A dual echo fast spin echo (FSE) sequence (repetition time (TR) 2000 ms, echo times (TE) 19/95 ms, 28 contiguous 5 mm axial slices covering the whole brain). (2) A MT sequence consisting of a MT pulse (duration 14.6 ms) applied before each slice of a 2D spoiled gradient echo sequence (TR 1180 ms, TE 12 ms, excitation flip angle 25°, field of view (FOV) 24 × 18 cm², slice thickness 5 mm. To minimize acquisition time a partial *k* space acquisition was used, collecting 48 phase encode steps to one side of *k*=0 and 8 to the other; this was reconstructed to a 256 × 256 matrix over a 24 × 24 cm² FOV). The interval between successive MT pulses was 41 ms. Ten independent measurements each consisting of 28 contiguous oblique axial slices covering the whole brain were made at differing MT pulse offsets and powers (three powers were used).⁹ (3) PD and T₁ weighted gradient echo data sets (TR/TE/flip angle: 1500 ms/11 ms/45° and 50 ms/11 ms/45°, respectively) permitting the calculation of T₁ relaxation time.¹⁷ An independent measurement of the observed T₁ relaxation time is required in order for *f* to be estimated. Total scan time was 1 hour.

Image processing

The first MT data set was used as a template to which the FSE images were registered (using the AIR package).¹⁸ The calculated T₁ relaxation map and other nine MT data sets were also registered to this template using mutual information registration.¹⁹ Lesions were then contoured on the FSE data set using DispImage (Plummer, Dept of Medical Physics and Bioengineering, UCL, UK) according to previously defined rules.²⁰ Fourteen normal appearing white matter (NAWM) regions and six normal appearing gray matter (NAGM) regions of interest (ROI) were also outlined on the first MT data set, with care taken to avoid lesion ROIs. ROIs in normal appearing regions were cylindrical and had a volume of 130 mm³ in the corpus callosum and internal capsule and 230 mm³

elsewhere. The following regions were outlined bilaterally in NAWM: frontal and occipital lobes, anterior and posterior limbs of the internal capsule, centrum semiovale and middle cerebellar peduncles. Single midline regions were outlined in the genu and splenium of the corpus callosum (see Figure 1). In gray matter, bilateral regions were placed in the thalamus, the caudate and the lentiform nucleus. Cortical gray matter regions were not used as partial volume artifact could not confidently be excluded.

The ROIs defined were then transferred to the 10 (coregistered) MT data sets and the T₁ map, and the model was fitted to values thus determined. Five fitted parameters (as previously defined,^{9,10}) were estimated: gM_0^A , RM_0^A , $f/(1-f)R_a$, $1/R_a T_{2a}$, and T_{2b} (via R_{rb}). Briefly, *g* is a constant reflecting scanner gain settings, M_0^A is the native magnetization of the free pool, *R* is the rate of cross relaxation between the two pools, R_a is the longitudinal relaxation rate constant of the free pool (the reciprocal of T_{1a}), T_{2a} is the T₂ of the free pool and R_{rb} is the absorption rate constant of the bound pool. Fitting was achieved with a least squares technique based on a Numerical

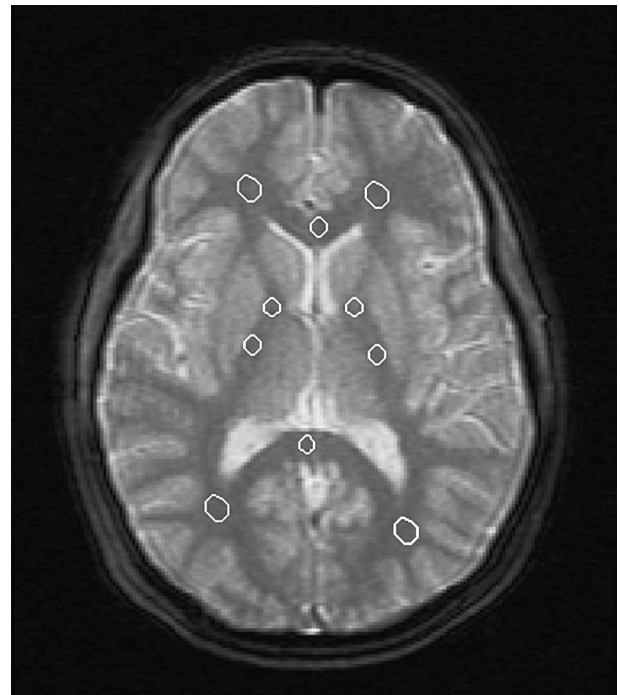


Figure 1 Regions of interest in a normal control placed (from top) in: frontal white matter, genu of the corpus callosum, anterior and posterior limbs of the internal capsule, splenium of the corpus callosum and occipital white matter.

Algorithms Group routine,²¹ and f was calculated from $f/(1-f)R_a$ using the observed T_1 , (which is related to R_a).⁹ R_b (the longitudinal relaxation rate constant of the bound pool) was fixed at 1 s^{-1} as the change in sum of squares with respect to R_b was zero. This means that R_b may take any value without changing the quality of fit and if R_b is unconstrained the model will not meaningfully converge. This is in accordance with Henkelman *et al.*³ who concluded that R_b could not be determined in such experiments. A value of 1 s^{-1} was selected since this was the value previously assumed,^{5,11} allowing data from this study to be compared more easily with data from previous work.

A super-Lorentzian line shape was assumed for the absorption line shape of the bound pool.⁵ The average of the root mean square residuals for parameter fitting in NAWM (patients and controls combined) was 1.2% (range 0.8% to 2.1%).

The same analysis was performed on a pixel by pixel basis in a single subject with MS. This permitted the generation of f and T_{2b} maps that provide a qualitative indication of the sensitivity of the parameters (see Figure 2).

Statistical analysis

Group comparisons, were made using the Mann–Whitney U test (SPSS11.0). Control and MS patient comparisons were made using a subset of patients below the age of 50 which allowed for better age and gender matching. The relationships between parameters were assessed using Spearman's rank correlation coefficient (r_s). The coeffi-

cient of variation was used as a measure of repeatability. P values of ≤ 0.05 were regarded as significant.

Results

Reproducibility

Five controls were imaged twice (mean time from scan to rescan was 42 weeks; range 21–70 weeks) and coefficients of variation for f and T_{2b} from NAWM were 5.4% and 4.7%, respectively.

Age and gender effects

There was no gender difference for either mean NAWM f or mean NAWM T_{2b} (patients and controls combined), $P=0.5$ and $P=0.8$, respectively. Age was inversely correlated with mean NAWM f ($r_s = -0.42$, $P < 0.001$) but not with mean NAWM T_{2b} ($r_s = 0.16$, $P = 0.13$).

Comparisons between patients and controls and correlations between parameters

Findings in lesions In lesions, mean f was 4.6 percent units (pu) versus 9.0 pu in control white matter, $P < 0.001$. Mean lesion T_{2b} was $11.5\ \mu\text{s}$ versus $10.6\ \mu\text{s}$ in control white matter, $P < 0.001$ (see Table 2).

Findings in NAWM, Deep gray matter and posterior fossa white matter In total NAWM, mean f was 8.0 pu in MS patients versus 9.0 pu in control white matter, $P < 0.001$. f values from separate white matter regions, deep grey matter

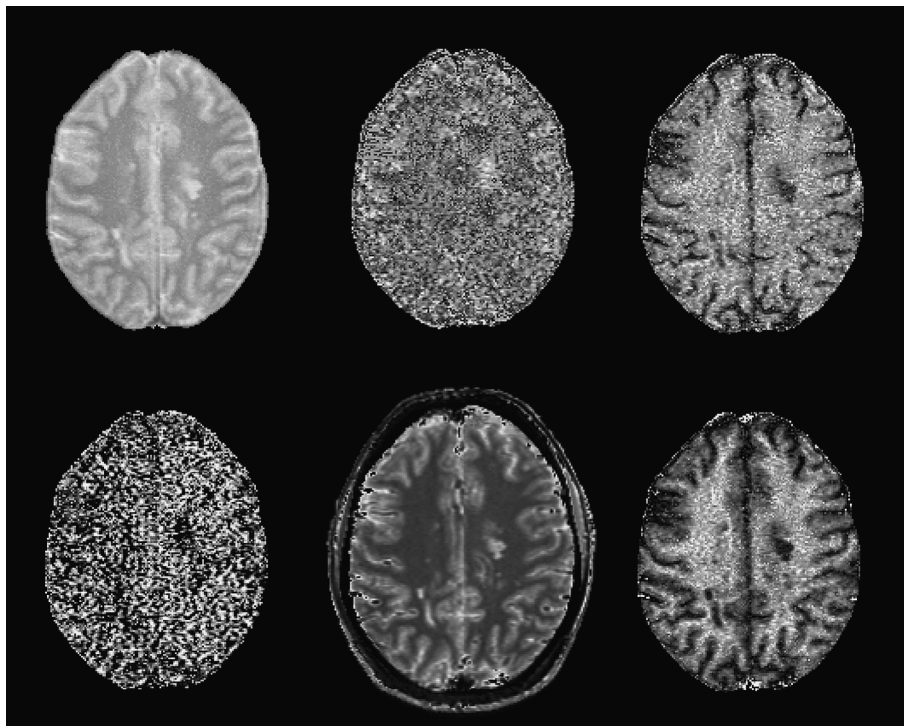


Figure 2 Parameter maps in a patient with MS. Top row from left to right: PD map, T_{2b} map, $f/(1-f)R_a$ map. Bottom row from left to right: T_{1a}/T_{2a} map, T_{1obs} map, f map.

Table 2 Lesion characteristics of the MS subgroups

	Mean lesion <i>f</i> (range)/pu	Mean lesion <i>T</i> _{2b} (range)/μs	Mean lesion <i>T</i> ₁ (range)/ms
Full MS cohort	4.7 (3.0–6.9)	11.5 (8.7–13.8)	980 (770–1210)
Relapsing–remitting MS	4.9 (3.4–6.9)	11.2 (8.7–13.4)	950 (820–1130)
Benign MS	4.4 (3.4–5.2)	12.1 (11.3–13.8)	1000 (940–1140)
Secondary progressive MS	4.4 (3.0–5.8)	11.6 (9.1–13.5)	1000 (840–1210)
Primary progressive MS	4.8 (3.6–6.5)	11.4 (9.7–13.4)	990 (770–1110)

regions and the cerebellar peduncles are shown in Table 3. *f* was abnormal in a number of these supratentorial white matter regions, but not in the middle cerebellar peduncles or deep gray matter.

*T*_{2b} was not significantly increased in total NAWM. *T*_{2b} values from separate regions are also given (Table 3) and the only significant increase seen was in occipital white matter. Comparing secondary progressive MS patients to controls revealed that *T*_{2b} was elevated in total NAWM (11.2 μs versus 10.6 μs, *P* = 0.03), occipital white matter (11.2 μs versus 10.6 μs, *P* = 0.01) and the splenium of the corpus callosum (11.6 μs versus 9.4 μs, *P* = 0.003). Such differences were not seen with other clinical subgroups.

In total NAWM, (MS patients and controls combined), *f* and *T*_{2b} were inversely correlated; *r*_s = -0.58, *P* < 0.001.

Cross relaxation rate in white and gray matter The cross relaxation term (*RM*₀^Δ), which provides an indication of the rate of cross exchange (*R*) between the bound and free pools, was found to be uniformly high in all regions in MS patients and controls (> 10⁵ s⁻¹).

Relationship between T₁ relaxation time and MT parameters

An estimate of the spin lattice relaxation time (*T*₁) was required in order for *f* to be estimated. Data on *T*₁ was derived from NAWM and lesions so that this data could be compared with *f* and *T*_{2b}. In comparison to controls,

*T*₁ was increased in lesions and in NAWM (Table 3). An inverse correlation was seen between *T*₁ and *f* in total NAWM (patients and controls combined); *r*_s = -0.80, *P* < 0.001 and a positive correlation was seen between *T*_{2b} and *T*₁; *r*_s = 0.32, *P* = 0.003.

T₂ lesion load measures

Mean *T*₂ lesion load was 19.3 ml (median 16.3 ml, range 0.5 to 79.3 ml). *T*₂ lesion load correlated with NAWM *T*_{2b} (*r*_s = 0.37, *P* = 0.004) and was inversely correlated with NAWM *f* (*r*_s = -0.52, *P* < 0.001)

Clinical status and correlations with MT parameters and T₁ relaxation time

Median EDSS and mean disease durations for all 60 subjects with MS and for the four clinical subgroups are given in Table 1. Table 4 shows all significant correlations between clinical function and MT measures. A modest correlation was seen between total NAWM *f* and the MSFC. *f* also correlated with the MSFC in several white matter tracts (the genu and splenium of the corpus callosum, the anterior limb of the internal capsule and the cerebellar peduncles). A modest correlation was seen in frontal NAWM. The only significant correlation between *f* and the EDSS was seen in the genu of the corpus callosum.

Table 3 *f*, *T*_{2b} and *T*₁ values compared between 33 MS patients and 27 healthy controls

Region	<i>f</i> /pu		<i>T</i> _{2b} /μs		<i>T</i> ₁ /ms	
	MS	Cont	MS	Cont	MS	Cont
Lesions^a	4.6*	9.0*	11.5*	10.6*	970*	650*
Total WM^b	8.0*	9.0*	10.8 ^{SP}	10.6 ^{SP}	710*	650*
Frontal WM	8.6*	9.8*	10.5	10.5	680*	610*
Genu of CC	8.1*	9.5*	10.8	10.6	700*	620*
Anterior IC	7.0	7.7	11.4	10.9	740	710
Posterior IC	8.0	8.2	11.3	11.6	730*	680*
Splenium of CC	8.4*	9.5*	10.0 ^{SP}	9.4 ^{SP}	730*	660*
Occipital WM	7.7*	9.1*	11.0^{SP}	10.6^{SP}	700*	630*
CSO	8.2*	9.2*	10.6	10.5	690*	630*
Cerebellar Ped.	7.4	7.4	10.4	10.2		
Total deep GM	4.6	4.7	10.7	10.6		
Caudate	3.6	3.6	10.8	11.1		
Lentiform	4.7	4.8	10.5	10.0		
Thalamus	5.6	5.6	10.9	10.6		

Bold: significant at *P* < 0.05 level; Bold*: significant at *P* < 0.01 using Mann–Whitney U test. Cont = values from 27 healthy controls, MS = values from 33 MS patients. WM = white matter, GM = gray matter, CC = corpus callosum, CSO = centrum semi ovale, IC = internal capsule. Cerebellar Ped. = middle cerebellar peduncle. ^a Lesions compared to total control white matter. ^b Supratentorial WM pooled. ^{SP} WM abnormal in SPMS versus controls (see text).

Table 4 Spearman's *r* values for clinical MR correlations

Region	<i>f/pu</i>		<i>T</i> _{2b} /μs		<i>T</i> ₁ /ms	
	EDSS	MSFC	EDSS	MSFC	EDSS	MSFC
Lesions	ns	ns	ns	ns	ns	ns
Total WM^a	−0.24	0.43*	ns	ns	ns	−0.28
Frontal WM	ns	0.30	ns	ns	ns	ns
Genu of CC	−0.34*	0.40*	ns	ns	0.32	−0.34
Anterior IC	ns	0.33	ns	ns	ns	ns
Posterior IC	ns	0.26	ns	ns	ns	ns
Splenium of CC	ns	0.38*	0.28	−0.34	0.24	−0.36*
Occipital WM	ns	0.25	ns	ns	ns	ns
CSO	−0.24	0.26	ns	ns	ns	ns
Cerebellar Ped.	ns	0.28	ns	ns		
Total deep GM	ns	ns	ns	ns		
Caudate	ns	ns	ns	ns		
Lentiform	ns	ns	ns	ns		
Thalamus	ns	ns	ns	ns		

Non bold: borderline only; *P* < 0.08. Bold: significant at *P* < 0.05 level. Bold* *P* < 0.01, ns: *P* > 0.08. WM = white matter, GM = gray matter, CC = corpus callosum, CSO = centrum semi ovale, IC = internal capsule. Cerebellar Ped. = middle cerebellar peduncle.
^a Supratentorial WM pooled.

*T*_{2b} showed a modest correlation with the MSFC (and EDSS) in the splenium of the corpus callosum (Table 4). *T*₁ correlated weakly with the MSFC in total NAWM. It also correlated with the MSFC and the EDSS in the corpus callosum (Table 4).

Discussion

In the study of MS, one limitation of conventional MRI is that it lacks the pathological specificity seen with histopathological techniques.^{6,7,22} Consequently, a MR technique that offers greater pathological specificity might improve upon the description or the monitoring of *in vivo* changes. A potential way of achieving this would be to use the magnetization transfer effect to derive a set of underlying parameters which, in turn, provide a more detailed description of tissue structure. Such an approach has been attempted here. This quantitative analysis of the MT effect yielded two parameters that provide complementary information. *T*_{2b}, a measure of the motional restriction of macromolecules, is increased in lesions whereas *f*, a measure of the macromolecular proton to total proton ratio, shows more diffuse but clinically relevant abnormality.

Although the nature of the macromolecular fraction is uncertain, the improvement seen in fitting when the model is altered to more accurately account for the nature of phospholipid bilayers,⁵ would suggest that phospholipid bilayers are an important component of the macromolecular content in this instance. The principle changes within lesions include T-cell mediated inflammation and demyelination,²³ although axonal loss,²⁴ and gliosis,²⁵ are also important features. In NAWM, axonal loss and gliosis (and, to a lesser extent, perivascular inflammation and demyelination) have also been demonstrated.^{26,27} Although *f* could be reduced by a decrease in the macromolecular content either via demyelination or ax-

onal loss, it should also be noted that *f* is a ratio of macromolecular protons to total protons and an increase in the free water component (as seen in edema) could also result in reduction in *f*. Histopathological studies correlating *f* with pathological findings are now required to test these hypotheses.

Correlations were seen between *f* and disability, particularly when *f* was estimated from long white matter tracts (the corpus callosum, the internal capsule and the cerebellar peduncles), indicating that the changes detected by this parameter do have clinical relevance. These correlations might suggest that long white matter tract pathology has a role in the accrual of disability.

*T*_{2b} was sensitive to pathology within lesions but was much less sensitive to abnormality within normal appearing brain tissue. The parameter is an estimation of the *T*₂ relaxation time of macromolecular protons and therefore is likely to detect changes to the structure of the macromolecular content (rather than changes to the macromolecular/free water ratio). The increase in *T*_{2b} in lesions and in the NAWM in SPMS patients suggests that there has been a change in the nature of the remaining macromolecules, conceivably due to a disruption of myelin and axonal phospholipid bilayers.

The results need to be interpreted in the context of a number of methodological considerations. Firstly, although the fitting of the model to experimental data is reasonable, (giving some confidence in its validity), the model contains a number of assumptions which are only partially met in practice. The assumption of two pools, made by both Henkelman and ourselves is itself an approximation, and a fuller description might include longer and shorter *T*₂ components in both the 'bound' and 'free' pools, along with interactions between them. The original model (proposed by Henkelman *et al.*⁸) also describes a system with a continuous saturating power and we have therefore made the assumption that our pulse sequence sufficiently approximates a continuous power. This might lead to some error in parameter accuracy and

although f and T_{2b} were similar when estimated with other models,^{11,12} it may explain the discrepancy in the rate of cross relaxation; (which was uniformly high in our case). A better estimation of the rate of cross relaxation might provide additional pathological insight and, with that in mind, we are continuing to refine the model and pulse sequence.

Secondly, the statistical analyses used did not correct for multiple comparisons and so it is possible that some of statistically significant results occurred by chance. For this reason the data has been presented in tabulated form so that the number of comparisons (and the proportion that are significant) can be appreciated. The pattern of abnormality seen in NAWM and the correlations with disability were similar between parameters, adding support to the view that these were biological effects.

The parameter f appears to be sensitive to abnormality within lesions and normal appearing brain tissue and its correlation with disability indicates that it has some clinical relevance. However, histopathological post mortem data is now required to assess the pathological specificity of f and T_{2b} . Imaging techniques that quantify demyelination would be of use in following MS pathology (for instance in symptomatic demyelinating lesions of the optic nerve or spinal cord) and especially in monitoring therapies to promote remyelination. Quantitative MT techniques are therefore likely to be the subject of further work, with the aim of refining the technique to improve upon specificity for the detection of myelin. Of note, Stanisz *et al.*²⁸ have recently found that the relative size of the bound pool (M_0^B), (estimated in rat sciatic nerve), altered in the presence of experimentally induced inflammation and demyelination. It will now be relevant to directly correlate f and T_{2b} with *post mortem* histopathological data and to obtain global *in vivo* measures via histogram analysis.

Acknowledgements

The authors thank D MacManus, R Gordon, C Benton, and the Multiple Sclerosis Society of Great Britain and Northern Ireland for their continuing support of the NMR Research Unit (including funding GRD and GJB during the course of this study). We would also like to thank all the people who kindly agreed to take part in this study.

References

- 1 van Buchem MA, Tofts PS. Magnetization transfer imaging. *Neuroimaging Clin N Am* 2000; **10**: 771–88.
- 2 Dousset V, Grossman RI, Ramer KN, Schnall MD, Young LH, Gonzalez-Scarano F *et al.* Experimental allergic encephalomyelitis and multiple sclerosis: lesion characterization with magnetization transfer imaging. *Radiology* 1992; **182**: 483–91.
- 3 Filippi M, Campi A, Dousset V, Baratti C, Martinelli V, Canal N *et al.* A magnetization transfer imaging study of normal-appearing white matter in multiple sclerosis. *Neurology* 1995; **45**: 478–82.

- 4 van Buchem MA, McGowan JC, Kolson DL, Polansky M, Grossman RI. Quantitative volumetric magnetization transfer analysis in multiple sclerosis: estimation of macroscopic and microscopic disease burden. *Magn Reson Med* 1996; **36**: 632–36.
- 5 Morrison C, Henkelman RM. A model for magnetization transfer in tissues. *Magn Reson Med* 1995; **33**: 475–82.
- 6 van Waesberghe JH, Kamphorst W, De Groot CJ, van Walderveen MA, Castelijns JA, Ravid R *et al.* Axonal loss in multiple sclerosis lesions: magnetic resonance imaging insights into substrates of disability. *Ann Neurol* 1999; **46**: 747–54.
- 7 Gareau PJ, Rutt BK, Karlik SJ, Mitchell JR. Magnetization transfer and multicomponent T2 relaxation measurements with histopathologic correlation in an experimental model of MS. *J Magn Reson Imaging* 2000; **11**: 586–95.
- 8 Henkelman RM, Huang X, Xiang QS, Stanisz GJ, Swanson SD, Bronskill MJ. Quantitative interpretation of magnetization transfer. *Magn Reson Med* 1993; **29**: 759–66.
- 9 Ramani A, Dalton C, Miller DH, Tofts PS, Barker GJ. Precise estimate of fundamental *in vivo* MT parameters in human brain in clinically feasible times. *Magn Reson Imaging* 2002; **20**: 721–31.
- 10 Tozer D, Ramani A, Barker GJ, Davies GR, Miller DH, Tofts PS. Quantitative magnetization transfer mapping of bound protons in multiple sclerosis. *Magn Reson Med* 2003; **50**: 83–91.
- 11 Sled JG, Pike GB. Quantitative imaging of magnetization transfer exchange and relaxation properties *in vivo* using MRI. *Magn Reson Med* 2001; **46**: 923–31.
- 12 Yarnykh VL. Pulsed Z-spectroscopic imaging of cross-relaxation parameters in tissues for human MRI: theory and clinical applications. *Magn Reson Med* 2002; **47**: 929–39.
- 13 Poser CM, Paty DW, Scheinberg L, McDonald WI, Davis FA, Ebers GC *et al.* New diagnostic criteria for multiple sclerosis: guidelines for research protocols. *Ann Neurol* 1983; **13**: 227–31.
- 14 Lublin FD, Reingold SC. Defining the clinical course of multiple sclerosis: results of an international survey. National Multiple Sclerosis Society (USA) Advisory Committee on Clinical Trials of New Agents in Multiple Sclerosis. *Neurology* 1996; **46**: 907–11.
- 15 Kurtzke JF. Rating neurologic impairment in multiple sclerosis: an expanded disability status scale (EDSS). *Neurology* 1983; **33**: 1444–52.
- 16 Fischer JS, Rudick RA, Cutter GR, Reingold SC. The Multiple Sclerosis Functional Composite Measure (MSFC): an integrated approach to MS clinical outcome assessment. National MS Society Clinical Outcomes Assessment Task Force. *Mult Scler* 1999; **5**: 244–50.
- 17 Parker GJ, Barker GJ, Tofts PS. Accurate multislice gradient echo T(1) measurement in the presence of non-ideal RF pulse shape and RF field nonuniformity. *Magn Reson Med* 2001; **45**: 838–45.
- 18 Woods RP, Mazziotta JC, Cherry SR. MRI-PET registration with automated algorithm. *J Comput Assist Tomogr* 1993; **17**: 536–46.
- 19 Studholme C, Hill DLG, Hawkes DJ. An overlap invariant entropy measure of 3D medical image alignment. *Pattern Recognit* 1999; **32**: 71–86.
- 20 Sailer M, O’Riordan JI, Thompson AJ, Kingsley DP, MacManus DG, McDonald WI *et al.* Quantitative MRI in patients with clinically isolated syndromes suggestive of demyelination. *Neurology* 1999; **52**: 599–606.
- 21 Ford B, Bentley J, Du Croz JJ, Hague SJ. The NAG library ‘machine’. *Softw Pract Exper* 1979; **9**: 65–72

- 22 Filippi M, Grossman RI. MRI techniques to monitor MS evolution: the present and the future. *Neurology* 2002; **58**: 1147–53.
- 23 Lassmann H. Neuropathology in multiple sclerosis: new concepts. *Mult Scler* 1998; **4**: 93–98.
- 24 Trapp BD, Peterson J, Ransohoff RM, Rudick R, Mork S, Bo L. Axonal transection in the lesions of multiple sclerosis. *N Engl J Med* 1998; **338**: 278–85.
- 25 Adams CWM. Pathology of multiple sclerosis: progression of the lesion. *Br Med Bull* 1977; **33**: 15–22.
- 26 Allen IV, McKeown SR. A histological, histochemical and biochemical study of the macroscopically normal white matter in multiple sclerosis. *J Neurol Sci* 1979; **41**: 81–91.
- 27 Evangelou N, Esiri MM, Smith S, Palace J, Matthews PM. Quantitative pathological evidence for axonal loss in normal appearing white matter in multiple sclerosis. *Ann Neurol* 2000; **47**: 391–95.
- 28 Stanisz GJ, Webb S, Munro CA, Pun T, Midha R. MR properties of excised neural tissue following experimentally induced inflammation. *Magn Reson Med* 2004; **51**: 473–79.